

Differences Between Stereocilia Numbers on Type I and Type II Vestibular Hair Cells

W. J. Moravec and E. H. Peterson

Department of Biological Sciences and Neuroscience Program, Ohio University, Athens, Ohio 45701

Submitted 27 April 2004; accepted in final form 13 June 2004

Moravec, W. J. and E. H. Peterson. Differences between stereocilia numbers on type I and type II vestibular hair cells. *J Neurophysiol* 92: 3153–3160, 2004. First published June 16, 2004; 10.1152/jn.00428.2004. A major outstanding goal of vestibular neuroscience is to understand the distinctive functional roles of type I and type II hair cells. One important question is whether these two hair cell types differ in bundle structure. To address this, we have developed methods to characterize stereocilia numbers on identified type I and type II hair cells in the utricle of a turtle, *Trachemys scripta*. Our data indicate that type I hair cells, which occur only in the striola, average 95.9 ± 16.73 (SD) stereocilia per bundle. In contrast, striolar type II hair cells have 59.9 ± 8.98 stereocilia, and type II hair cells in the adjacent extrastriola average 44.8 ± 10.82 stereocilia. Thus type I hair cells have the highest stereocilia counts in the utricle. These results provide the first direct evidence that type I hair cells have significantly more stereocilia than type II hair cells, and they suggest that the two hair cell types may differ in bundle mechanics and peak mechano-electric transduction currents.

INTRODUCTION

Vertebrates use mechanoreceptors called hair cells to detect head motion. Each hair cell bears a hair bundle comprising a single kinocilium and multiple stereocilia. There are two types of vestibular hair cells. Type II hair cells are innervated by bouton terminals of vestibular primary afferents; they occur in all vertebrates. Type I hair cells are innervated by cup-like, calyceal terminals; they occur only in amniotes (reptiles, birds, and mammals). These two hair cell types were recognized almost 50 years ago (Wersäll 1956), but their distinctive functional roles are still poorly understood.

Hair cells are mechanoreceptors; thus one logical suggestion is that type I and type II hair cells differ in bundle mechanics. Because bundle structure is a major determinant of bundle mechanics (Howard et al. 1988; Peterson et al. 1996; Silber et al. 2003), we compared the morphology of type I and type II ciliary bundles. Here we describe a method that allows us to characterize stereocilia numbers on identified hair cell types. We report, for the first time, that type I hair cells have significantly higher stereocilia numbers than type II hair cells. These differences in stereocilia counts suggest that type I and type II hair cells may differ in bundle mechanics and peak mechano-electric transduction currents.

Our experimental preparation is the utricle of a turtle, *Trachemys (Pseudemys) scripta elegans*. In this species, type I hair cells are restricted to the striola (Jorgensen 1974, 1988), a crescent-shaped specialization in the neuroepithelium and oto-

conial membranes of vertebrate otolith organs (Werner 1933). Previously (Peterson and Rowe 2001), we reported that the striola of *T. scripta* can be distinguished from the extrastriola by quantitative features of its ciliary bundles and that it is subdivided into two parallel bands, which we call zone 2 and zone 3 (Fig. 1A). Zone 3 bundles vary markedly in stereocilia numbers; some of them have the highest stereocilia counts in the utricle (Peterson and Rowe 2001). Type I hair cells are restricted to zone 3, and indirect evidence (based on cuticular plate size) suggested the hypothesis that bundles with the highest stereocilia counts belong to type I hair cells (Moravec et al. 2003). To test this hypothesis, we used confocal microscopy to examine utricular whole mounts that were double-stained to visualize stereocilia and the utricular afferents that define hair cell type. Some of these data have appeared previously in abstract form (Moravec and Peterson 2004).

METHODS

Four turtles of both sexes (11–13 cm plastron length, 225–329 g; Kons Direct, Germantown, WI; Table 1) provided useful data. Animal care protocols have been published previously (Brichta and Peterson 1994). We followed the Ohio University Animal Care and Use Committee guidelines at all times.

Labeling of primary afferents and hair bundles

We chilled turtles in an ice bath for 15–30 min and killed them via intramuscular injection of 0.7 ml pentobarbital sodium with phenytoin sodium (Euthasol). We decapitated the turtles, bisected the heads, placed them in oxygenated turtle Ringer solution (Houngaard and Nicholson 1990), and removed the brains from the skulls, leaving the labyrinth and a large stump of cranial nerve VIII (CN8) intact.

We labeled afferents by applying gelfoam pellets infiltrated with Micro-Ruby (BDA/Rhodamine 3,000 mW, Molecular Probes; 33 mg/ml in distilled water) to the stump of CN8 and maintained the head in circulating, oxygenated Ringer solution. After 4–6 h, we fixed the heads with 4% paraformaldehyde in phosphate buffer for 24 h, removed the utricles from the bony labyrinths, opened them, and removed the otolithic membranes. We visualized stereocilia with phalloidin, which labels filamentous actin, conjugated to Alexa-Fluor 488 (Molecular Probes; 2U/100 ml 0.1 M phosphate buffer). Finally, we mounted intact utricles on microscope slides that had wells filled with anti-fade reagent (Glycerol/PBS, Molecular Probes) and secured them with coverslips.

To judge whether the band of calyces was adequately labeled, we compared Micro-Ruby-labeled utricles with utricles from a separate study in which we used a different technique to visualize calyces. In that study, we manipulated the bath composition to swell calyces so

Address for reprint requests and other correspondence: E. H. Peterson, Dept. Biological Sciences, Irvine Hall, Ohio Univ., Athens, OH 45701 (E-mail: peterson@ohiou.edu).

The costs of publication of this article were defrayed in part by the payment of page charges. The article must therefore be hereby marked “advertisement” in accordance with 18 U.S.C. Section 1734 solely to indicate this fact.

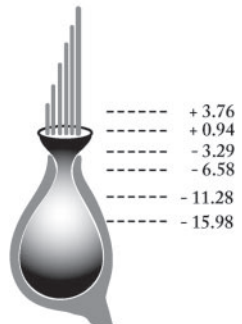
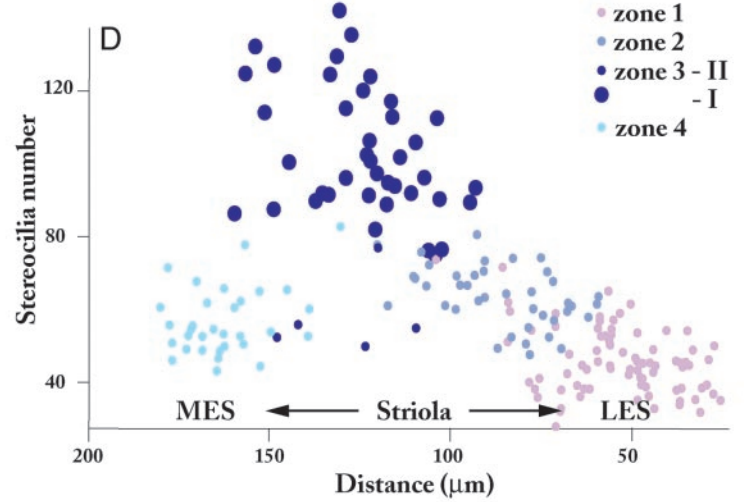
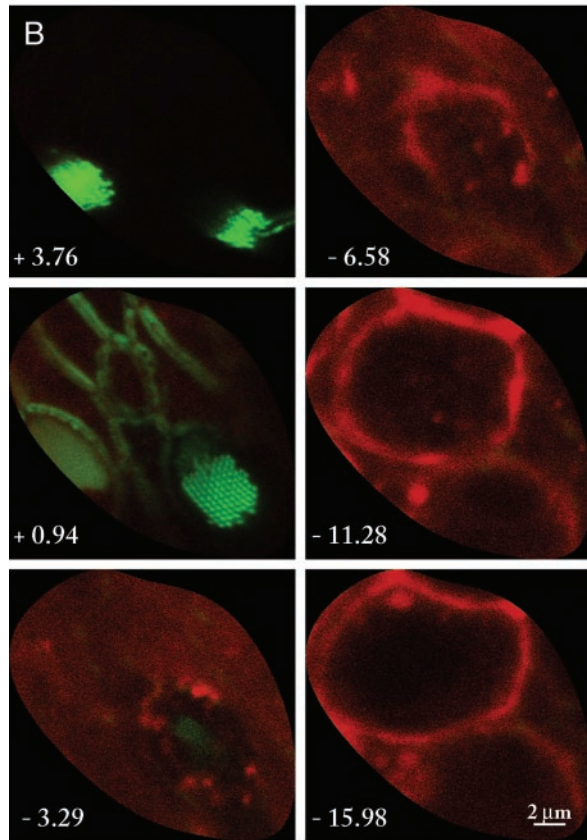
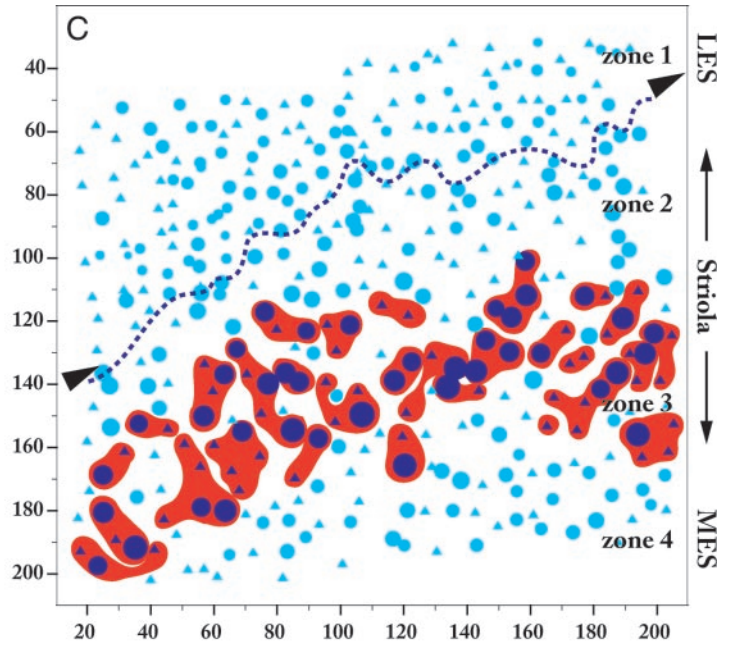
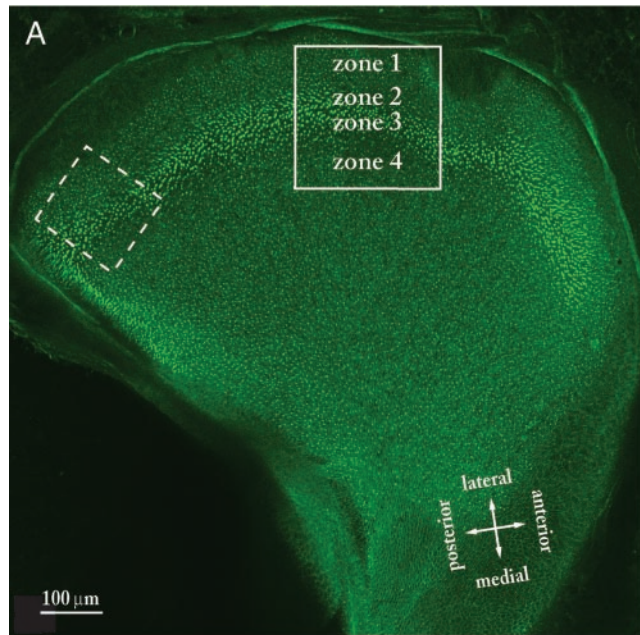


TABLE 1. *Stereocilia numbers on utricular hair cells from four primary samples*

	Type II					Type I (zone 3)
	Zone 1	Zone 2	Zone 3	Zone 4	All zones	
Turtle 1 (<i>n</i> = 77)					54.9 ± 11.58 (33–76) <i>n</i> = 52	90.7 ± 19.09 (60–130) <i>n</i> = 25
Turtle 2 (<i>n</i> = 20)		62.5 ± 8.96 (48–72) <i>n</i> = 8	30 <i>n</i> = 1		51.7–58.2 58.9 ± 13.70 (30–72) <i>n</i> = 9	82.8–98.6 91.5 ± 13.40 (72–118) <i>n</i> = 11
Turtle 3 (<i>n</i> = 102)	40.5 ± 11.08 (8–64) <i>n</i> = 48	62.0 ± 8.49 (34–75) <i>n</i> = 23	59.1 ± 8.29 (47–73) <i>n</i> = 8	58.2 ± 5.54 (52–67) <i>n</i> = 5	49.3 ± 14.12 (26–72) <i>n</i> = 84	100.7 ± 14.44 (78–129) <i>n</i> = 18
Turtle 4 (<i>n</i> = 198)	37.3–43.8 43.3 ± 9.26 (26–72) <i>n</i> = 81	58.4–65.7 59.8 ± 8.11 (45–76) <i>n</i> = 40	52.2–66.1 54.4 ± 9.71 (47–71) <i>n</i> = 5	51.3–65.1 53.0 ± 8.87 (41–77) <i>n</i> = 32	46.2–52.3 49.8 ± 11.33 (26–72) <i>n</i> = 158	93.5–107.8 98.1 ± 16.37 (71–136) <i>n</i> = 40
All turtles (<i>n</i> = 397)	41.2–45.3 42.3 ± 10.02 (8–72) <i>n</i> = 129	57.2–62.4 60.8 ± 8.29 (34–76) <i>n</i> = 71	42.3–66.5 55.4 ± 11.16 (30–73) <i>n</i> = 14	49.8–56.2 53.7 ± 8.62 (41–77) <i>n</i> = 37	48.0–51.6 50.8 ± 12.46 (8–77) <i>n</i> = 303	92.9–103.3 95.9 ± 16.73 (60–136) <i>n</i> = 94
	40.5–44.0	58.9–62.8	48.9–61.8	50.8–56.6	49.4–52.2	92.4–99.3

Values are mean ± SD, range, number of measured hair cells, and 95% CIs of the mean.

that they appear as a band of black rings surrounding one to seven hair cells in utricular whole mounts (Moravec et al. 2003). We analyzed utricles only if the band of calyces appeared to be fully labeled.

Confocal microscopy

We used a Zeiss LSM 510 confocal microscope equipped with a Plan-Apochromat 63× oil immersion DIC objective (NA = 1.4) to collect all image stacks, and we controlled on-screen image size via digital magnification. Pinhole size varied from 0.60–0.75 Airy units, which yielded optical sections 0.4–0.6 μm thick. In the first two turtles, we visualized hair bundles and afferents in the same stacks using digitally magnified multi-track scans with 488- and 543-nm

laser lines (Fig. 1B) (see Supplemental Material¹ for confocal stack). In the final two turtles, we also mapped the spatial location of all hair cells in our sample area as follows. First, we made a low-magnification, multi-track image stack of our sample area with 488- and 543-nm laser lines, including all bundles and afferents. Then we used single-track scans with the 488-nm laser to acquire higher magnification images of small groups of bundles within the sample area. Next we combined four to six of these higher magnification confocal stacks to form a montage of the total sample area. Finally, we used MATLAB (ver. 6.5; MathWorks) to convert the coordinates of hair cells in individual high magnification images to a single set of global coordinates.

¹ The Supplemental Material for this article (a video) is available online at <http://jn.physiology.org/cgi/content/full/00428.2004/DC1>.

FIG. 1. Hair bundles in the striola and adjacent extrastriola of turtle utricle. *A*: confocal projection of a left turtle utricle stained with the actin probe phalloidin to visualize hair bundles. All 4 primary samples (Table 1) were collected from the region outlined by a solid box; it includes the striola, which has larger bundles and so appears brighter, and adjacent lateral and medial extrastriola. The striola is subdivided into parallel zones 2 and 3; zones 1 and 4 correspond to the adjacent lateral and medial extrastriola, respectively. We also sampled a region straddling the far posterior striola (dotted box) to test whether differences between hair cell types were specific to our primary sample area (solid box) or a more general feature of the utricular macula. *B*: 6 optical sections from a confocal stack through a type I hair cell; the complete stack is included as Supplemental Material. Bundles are labeled with phalloidin conjugated to Alexa Fluor 488; they appear green. Afferents are labeled with Micro-Ruby; they appear red. Numbers in the bottom left corner of each image show the level of the optical section in micrometers relative to the approximate apical surface of the hair cell (level 0). The complete stack comprised 50 sections; step size was 0.47 μm. We counted stereocilia in a higher magnification view of level +0.94. Examples of such higher magnification views are shown in Fig. 2. The narrow neck of the calyx is visible at level -6.58; the diameter of the calyceal terminal increases at deeper levels (-11.28, -15.98). *Inset*: schematic type I hair cell and its postsynaptic calyx. Numbers at the right indicate the approximate position of each optical section. *C*: *x-y* plot showing the location and relative stereocilia numbers of all hair bundles from 1 data set (turtle 4; Table 1). Each symbol shows the location of 1 bundle. *x*- and *y*-axes are in micrometers from an arbitrary origin. Zone 1 corresponds to the lateral extrastriola (LES); zone 4 corresponds to the medial extrastriola (MES); the striola comprises zones 2 and 3. Circles are measured bundles; circle area is scaled to stereocilia number. Triangles are bundles too distorted to measure accurately. The band of labeled calyces (red profiles) defines zone 3; it is displaced 20–30 μm from the line of polarity reversal (dotted line). Comparison of measured type I bundles (dark blue circles) with measured type II bundles (light blue circles) suggests that type I hair cells have more stereocilia than type II hair cells. Arrowheads indicate approximate viewing direction for the plot in *D*. *D*: data from *C* are replotted to show type- and region-specific differences in stereocilia number more clearly. The image was created in 2 steps. First, we constructed an *xyz* scatterplot, where *x*- and *y*-axes represent bundle position (as in *C*), and the *z*-axis represents stereocilia number. We rotated the 3-dimensional plot so that the *z*-axis (stereocilia number) is vertical, the data cloud is viewed from the *y*-axis, approximately parallel to the line of polarity reversal (*C*, arrowheads), and the *x*-axis is collapsed onto this *yz*-plane. Bundles from each zone are identified by different colors. Symbols for different zones sometimes overlap on the abscissa. This occurs because zone borders are irregular; e.g., when viewing along a line between the 2 arrowheads in *C*, above, one encounters bundles in zones 1 and 2. Note that, in zone 3, type I hair cells (large, dark blue symbols) generally have higher stereocilia counts than type II hair cells (small, dark blue symbols).

dinates that showed the location of all hair cells within our total sample area. To do this, we 1) selected the region to be magnified and recorded the location of its upper left corner on the low-magnification image, 2) specified the location of each cell within the high magnification image as a vector originating in the upper left corner of that image and ending at the kinocilium, 3) rescaled the vector magnitude in proportion to the magnification ratio between the low- and high-magnification images, and 4) translated the origin of the vector to its correct location on the low-magnification image. High-magnification stacks provided the clearest images of hair bundles; the low-magnification stack allowed us to determine the hair cell type for each bundle. An example of one such data set is shown in Fig. 1C.

Except for one control sample (see *Control for the effect of sample location*), all analyses focused on an $\sim 200 \times 200\text{-}\mu\text{m}$ region of interest (Fig. 1A, solid box) that included the striola (zones 2 and 3) and adjacent lateral (zone 1) and medial (zone 4) extrastriola. We refer to this as our primary sample area. We counted stereocilia in this region because type I hair cells are located in the striola (Jorgensen 1974, 1988; Moravec et al. 2003) and because it is important to contrast stereocilia numbers on type I hair cells with stereocilia numbers on type II hair cells at the same utricular locus (see *Known location*). Our primary sample area is part of the larger transect on which we focus much of our quantitative analyses of bundle structure (Fontilla and Peterson 2000). Data for our four primary samples are summarized in Table 1.

Measurements and statistical analysis

For hair cells that had bundles clear enough to analyze, we counted stereocilia in optical sections just above the apical surface, directly from the computer monitor. We examined more than one optical section through the base of the bundle if necessary to visualize all stereocilia in the bundle; this is useful if the hair cell surface is curved or not perfectly perpendicular to the scanning axis. We also recorded hair cell type based on the presence or absence of a calyx, the cup-like afferent terminal that surrounds each type I hair cell (Fig. 1B, inset). For turtle 1, we recorded stereocilia numbers and hair cell type only; for turtles 2–4, we also assigned hair cells to one of four zones (Fig. 1, A and C; Table 1). In this paper, zone 1 corresponds to hair cells lateral to the line of polarity reversal (dotted line in Fig. 1C); the kinocilial (tall) ends of utricular bundles face each other across this reversal line. Occasionally, bundles with striolar-like properties, i.e., relatively high stereocilia counts (this report) and low kinocilia-to-stereocilia height ratios (Xue and Peterson 2004) occur immediately lateral to the line of polarity reversal (see Fig. 7 of Fontilla and Peterson 2000). Such bundles properly belong in zone 2 rather than zone 1 (i.e., they should be considered striolar bundles). Because we have not yet developed quantitative criteria for identifying these “errant” striolar bundles, we made no attempt to separate them from the rest of zone 1 in this report. Thus differences we describe between zone 1 (lateral extrastriolar) and zone 2 (striolar) bundles are probably underestimates of the true difference between these two bundle populations. Zone 2 corresponds to hair cells between the reversal line and the band of calyces. Zone 3 corresponds to hair cells innervated by calyces and any hair cells scattered between the calyceal terminals. Collectively, zones 2 and 3 form the striola. Zone 4 corresponds to hair cells medial to the band of calyces.

All four zones contain type II hair cells; type I hair cells are restricted to zone 3 (Moravec et al. 2003). We tested differences between stereocilia numbers for statistical significance using ANOVA and planned or posthoc (Tukey honest significant difference test for unequal sample sizes) comparisons.

Control for the effect of sample location

To ensure that any differences between type I and type II striolar bundles are not unique to our primary sample area (Fig. 1A, solid

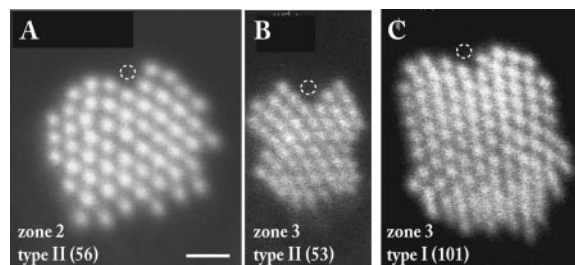


FIG. 2. Three bundle populations in the striola. Images are single optical sections through the base of each bundle; we used such images to count stereocilia. Zone assignment and hair cell type are indicated in the bottom left corner of each image. Stereocilia numbers for each array are shown in parentheses; they are typical of their respective bundle populations (Table 1). Dotted profiles show approximate position of kinocilia. Scale for all 3 micrographs: 1 μm .

box), we also sampled the far posterior striola in turtle 4 (Fig. 1A, dotted box).

RESULTS

In agreement with earlier results (Moravec et al. 2003), labeled calyces formed a 50- to 60- μm -wide band that followed the trajectory of the striola and was displaced 20–30 μm medially from the line of polarity reversal (Fig. 1C). This distribution corresponds to zone 3 as identified from autocorrelation analysis (Rowe and Peterson 2004) of scanning micrographs (Peterson and Rowe 2001). Thus type I hair cells are restricted to striolar zone 3. Stereocilia numbers on hair cells of the striola and adjacent extrastriola were markedly heterogeneous. This is shown for one utricle in Fig. 1, C and D, and summarized for all four cases in Table 1. High magnification confocal micrographs of type I and type II bundles from the striola are shown in Fig. 2. A second type I bundle and its calyx terminal are shown in Fig. 1B and in Supplemental Material.

A two-factor ANOVA revealed significant effects of hair cell type ($F = 171.7$, $df = 1, 315$, $P < 0.001$) and of zone ($F = 46.5$, $df = 3, 315$, $P < 0.001$). Thus there are significant differences between type I and type II hair cells (collapsed across zones) and between zones (collapsed across hair cell types). The R^2 value for the overall model ($R^2 = 0.79$; $F = 289$, $df = 4, 315$, $P < 0.001$) indicates that differences between hair cell type and utricular zone account for a significant percent (79%) of the variability in stereocilia number within our primary sample area. We can partition these overall differences in stereocilia number into two sources of variation.

Type I hair cells have significantly more stereocilia than total striolar type II hair cells (95.9 ± 16.7 , $n = 69$ vs. 59.9 ± 9.0 , $n = 85$; $F = 597.5$, $df = 1, 215$, $P < 0.001$) or type II cells within zone 3 alone (55.4 ± 11.2 , $n = 14$; $F = 94.1$, $df = 1, 81$, $P < 0.001$; Figs. 2 and 3A, filled symbols, and 3B). To control for the possibility that these differences between type I and type II stereocilia numbers are unique to our primary sample location (Fig. 1A, solid box) we compared stereocilia numbers on type I and type II hair cells from a sample at the far posterior striola (Fig. 1A, dotted box; Fig. 3A, open symbols). In this region, stereocilia numbers are nearly identical to those in our primary sample area. Type I hair cells averaged 97 ± 12.6 stereocilia ($n = 26$; range, 80–119); these stereocilia counts are significantly higher than total striolar type II cells in the posterior striola (57.2 ± 7.9 , $n = 91$, range, 44–74; $F =$

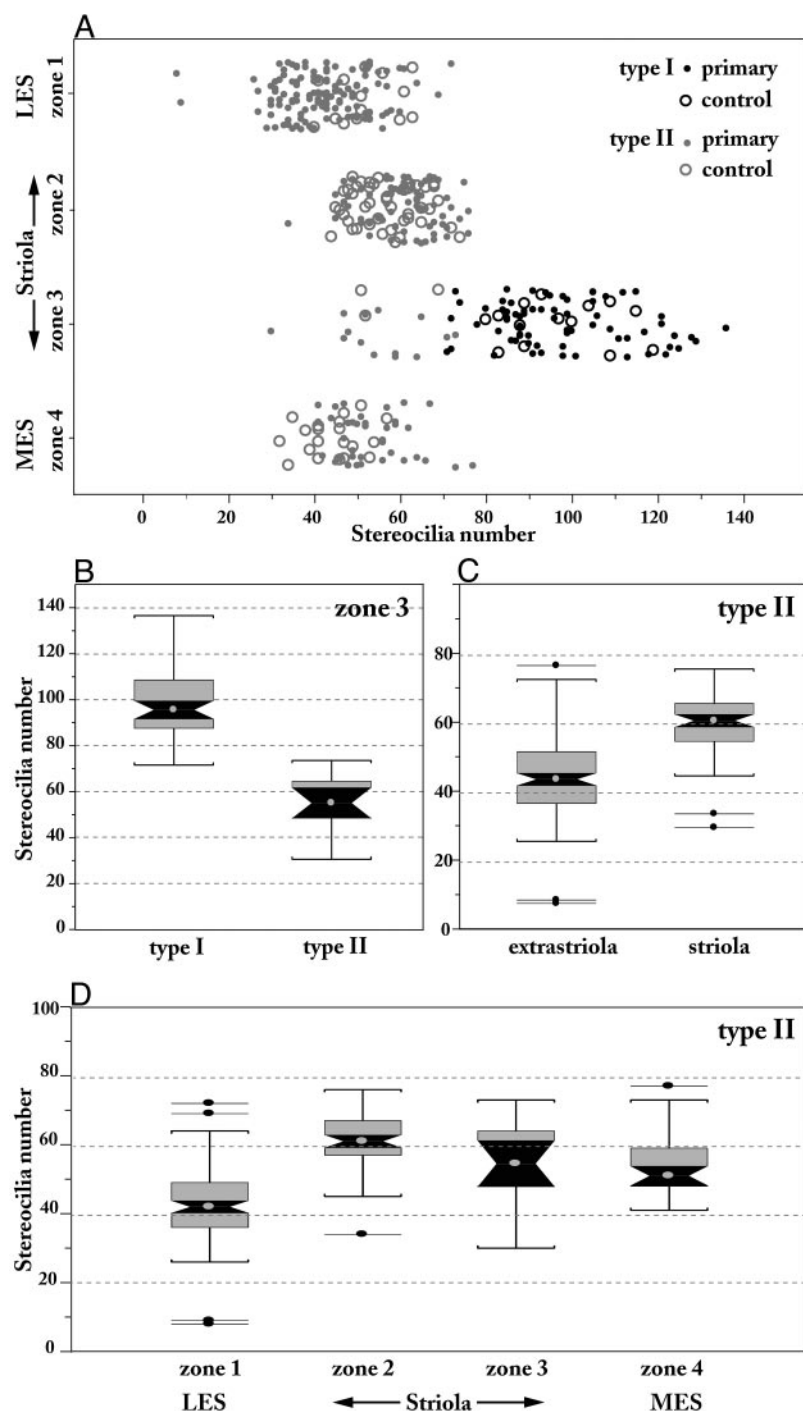


FIG. 3. Type- and region-specific differences in stereocilia numbers for 3 utricles in which hair cells were assigned to utricular zones (Table 1, turtles 2–4). *A*: dot plot showing the number of stereocilia on 320 measured hair bundles from the primary sample area in 3 turtles as a function of utricular zone (turtles 2–4; solid symbols). Data points have been jittered along the ordinate for clarity. Within zone 3, type I bundles (dark symbols) and type II bundles (light symbols) have significantly different stereocilia counts. Open circles represent 97 measured bundles from a control sample in far posterior utricle (Fig. 1*A*, dotted box). For this control sample, type I and type II bundles in zone 3 have significantly different stereocilia counts. *B*: box plot summarizing differences between stereocilia numbers on type I and type II hair cells within zone 3. Dots, medians; gray boxes, interquartile range; black boxes, 95% CIs of the median; whiskers, $1.5 \times$ interquartile range; isolated points, outliers. Nonoverlapping CIs indicate statistically significant differences between the 2 groups. *C*: box plot summarizing differences between stereocilia numbers on striolar and extrastriolar type II hair cells. Box plot conventions as in *B*. Nonoverlapping CIs indicate that stereocilia counts for the 2 populations are significantly different. *D*: box plots summarizing region-specific differences in stereocilia number for type II hair cells. Stereocilia numbers on type II hair cells are lowest in zone 1; they peak in zone 2 and decline slightly, but significantly, from zone 2 to zone 4. Nonoverlapping CIs indicate statistically significant differences between zones. CI for zone 3 is large because there are relatively few type II hair cells in zone 3 (Table 1).

208.6, $df = 1, 61, P < 0.001$) or type II hair cells in zone 3 alone ($57.3 \pm 10.1, n = 9$, range, 51–69; $F = 25.7, df = 1, 15, P < 0.001$). Thus the difference between stereocilia numbers on type I and type II hair cells appears to be a general feature of the utricular striola in *T. scripta*.

A second source of variation in stereocilia number arises from local differences in type II hair cells (Fig. 3, *A, C*, and *D*). A single-factor ANOVA on type II hair cells revealed that striolar type II hair cells have significantly more stereocilia than hair cells in the adjacent lateral and medial extrastriola (Fig. 3*C*; planned comparison: $F = 38.3, df = 1, 247, P < 0.001$). In addition, there is a significant effect of zone on

stereocilia number (Fig. 3*D*; $F = 63.7, df = 3, 247, P < 0.001$). The R^2 value for the overall model was 0.44, indicating that zone assignment accounts for 44% of the variability in type II stereocilia numbers. Stereocilia number increased significantly from zone 1 (lateral extrastriola) to striolar zone 2 (posthoc comparison, $P < 0.001$) then decreased toward the medial extrastriola (zone 4). Comparison of type II bundles in zones 2–4 indicated that there were no significant differences between adjacent zones (zone 2 vs. 3, zone 3 vs. 4), but the difference between zone 2 and zone 4 was significant (posthoc comparison, $P < 0.01$), as was the regression of stereocilia number against zones 2–4 ($F = 17.1, df = 1, 120, P < 0.001$;

$R^2 = 0.12$). Thus stereocilia numbers on type II hair cells peak in zone 2 and decrease toward both the lateral and medial extrastriola.

DISCUSSION

Our most important finding is that utricular type I hair cells have more stereocilia than type II hair cells. In addition, type II hair cells in or near the striola differ in stereocilia numbers as a function of their location. To show these differences between bundles, we attempted to satisfy four criteria.

Accurate measurement

Approximately 50% of bundles in our samples were measurable. We did not count stereocilia on the remaining bundles because they were bent off the optical axis of the microscope, which made it more difficult to resolve their closely spaced stereocilia.

Adequate sample size

Convincing demonstration of differences between bundles requires samples that are large enough for statistical analysis. In our primary sample area (Fig. 1A, solid box), which includes the striola and adjacent lateral and medial extrastriola, we counted stereocilia on 397 bundles from four utricles of four different turtles. For three of these utricles ($n = 320$), we also assigned type II hair cells to a utricular zone (by definition, type I hair cells are always in zone 3). All the type- and location-specific differences we report here were statistically significant with one exception: medial to the reversal line, type II bundles in adjacent zones did not differ in stereocilia counts. Nevertheless, the gradual decrease in stereocilia numbers from zone 2 to zone 4 was significant. In addition to our four primary samples (Table 1), we also counted stereocilia numbers on 97 hair cells from the far posterior striola (Fig. 1A, dotted box). In this control sample, stereocilia numbers on type I and type II hair cells were also significantly different (Fig. 3A, open circles).

Known location

Knowledge of hair cell location is critical for establishing type-specific differences in ciliary bundles. The reason for this is that bundle structure is known to vary with location in amniote vestibular organs (e.g., Jorgensen 1989; Kirkegaard and Jorgensen 2001; Lim 1976, 1979; Lindeman 1969; Peterson et al. 1996), and without holding location constant, it is impossible to know whether observed differences between type I and type II bundles are due to effects of spatial locus or effects of hair cell type. In turtle utricle, type I hair cells have significantly more stereocilia than type II hair cells, even when location is held constant (i.e., when all measured bundles are within the striola or even within zone 3). Thus the differences we observed between hair cell types are not confounded by spatial effects.

Accurate identification of hair cell type

We identified hair cell type by labeling postsynaptic afferents with a dextran amine tracer applied to the utricular nerve.

We cannot exclude the possibility that we missed some type I hair cells because their calyces were too weakly labeled, but we believe the number of such misidentified hair cells is small for two reasons. First, we analyzed only those utricles in which the band of calyces was judged to be completely labeled (compared with an alternate method of visualizing calyces; see METHODS). Second, the pattern of afferent labeling and the differences in stereocilia numbers between hair cell types were remarkably consistent in all four cases (Table 1); such consistency is unlikely if a significant number of type I hair cells were misidentified. Note too that the type I–type II differences in stereocilia counts were so large that a small number of misidentified type I cells, if there were any, would not be likely to change the results of our statistical analysis. One advantage of labeling afferents with dextran amine is that individual calyceal terminals can be isolated (Fig. 1C, red profiles), the number of type I hair cells supplied by each terminal can be counted, and the structural features of their bundles can be analyzed.

A previous study on Daubenton's bat reported statistically significant differences between stereocilia numbers on striolar and extrastriolar hair cells (Kirkegaard and Jorgensen 2001); in contrast to the present results, striolar bundles in the bat had significantly *fewer* stereocilia than extrastriolar bundles. Two other studies have suggested that type I hair cells may have more stereocilia than type II hair cells based on indirect evidence: comparisons of a mixed population of bundle types with a population of known type II bundles (Peterson et al. 1996) or extrapolations from partial stereocilia counts (Morita et al. 1997). To our knowledge, the present results are the first direct demonstration of significant differences in stereocilia numbers on type I and type II hair cells of any vestibular organ. The picture that emerges is of two superimposed patterns.

Type I hair cells are restricted to one subdivision of the striola, and they form a distinct population because of their high stereocilia counts. We saw no obvious tendency for type I hair cells supplied by the same calyceal terminal to have similar stereocilia counts or for stereocilia numbers to depend on the number of type I receptors supplied by a single calyceal terminal. This result is tentative, however, because often the type I hair cells supplied by a single calyceal terminal were not all measurable with our current techniques (Fig. 1C).

Type II hair cells are present throughout the striola and adjacent extrastriola. Their stereocilia numbers peak just medial to the line of polarity reversal (zone 2) and decrease significantly toward both the lateral and medial extrastriola. The numbers we report for type II hair cells in zones 1 and 4 (Table 1) are typical of type II hair cells in lateral and medial extrastriola. We base this on results of a separate study in which we used scanning micrographs of sonicated utricles and autocorrelation analysis (Rowe and Peterson 2004) to analyze stereocilia arrays (number, spacing, and arrangement of stereocilia on the apical surface of individual hair cells) along a medial-to-lateral strip of macula; this strip includes the primary sample area described in the present report. Data from such sonicated utricles suggest that stereocilia numbers do not vary significantly across either subdivision of the extrastriola except for a slight decrease in the peripheral 25 μm of the lateral extrastriola (Peterson and Rowe 2001; Peterson and M. H. Rowe, unpublished data). We conclude that 1) type I hair cells have

higher stereocilia numbers than striolar type II hair cells, 2) striolar type II hair cells have higher stereocilia counts than type II hair cells in the extrastriola, and therefore, 3) type I hair cells have the highest stereocilia numbers in the utricle.

We considered the possibility that the small type II hair cells in zone 3 (Fig. 2B) represent developing bundles, but this seems unlikely for three reasons. First, we and others (Severinsen et al. 2003) have observed apparently immature bundles in turtle utricle, and they are unlike type II bundles in zone 3 because they appear to have fewer stereocilia, smaller apical surfaces, and shorter kinocilia and stereocilia (Xue and Peterson 2004). Second, such apparently immature bundles are more prevalent in the lateral and medial extrastriola than in the striola. This is consistent with observations that bundles are added to the utricular macula much more frequently in the extrastriola than in the striola (cf. Fig 6b of Severinsen et al. 2003). Third, as noted above, type II bundles in zone 3 appear to be part of a gradient in which stereocilia numbers decrease (present results) and the ratio of kinocilia to stereocilia heights increases (Xue and Peterson 2004) from striolar zone 2 into the medial extrastriola.

Stereocilia numbers matter because they affect bundle mechanics and transduction currents. The stiffness of a ciliary bundle, and thus the range of head accelerations it encodes, is approximated by the formula

$$K = \sum_{i=1}^N k_i$$

where K is the static linear stiffness of the bundle, N is the number of stereocilia in the bundle, and k is the linear stiffness of a single stereocilium (Howard et al. 1988). Thus stereocilia number is a major (but not the only) determinant of bundle stiffness. Preliminary models of turtle utricular bundles confirm this effect of stereocilia number on steady-state stiffness (Silber et al. 2004).

Stereocilia number is also likely to affect transduction current amplitudes because each stereocilium is associated with one to two mechanotransduction channels (Denk et al. 1995). Interestingly, a preliminary report suggests that peak mechanoelectric transduction currents in type I hair cells of turtle utricle are 492 ± 216 pA compared with 149 ± 47 pA for striolar type II hair cells (Rennie and Ricci 2004). It is unclear why this difference in transduction currents ($>3:1$) is greater than the difference in stereocilia counts ($<2:1$); possible reasons include sampling bias and differences in the number of channels per stereocilium or in single transduction channel currents. In turtle auditory hair cells, single channel currents depend on the Ca^{2+} concentration of the bathing medium, and they decrease with the characteristic frequency of the hair cell (Fig. 5 of Ricci et al. 2003). If this frequency dependence extrapolates to the response range of turtle vestibular hair cells, one would predict a channel current of $<3-7$ pA (depending on Ca^{2+} concentration) for these low-frequency receptors and a maximum transduction current of 300–700 pA for type I hair cells (assuming 100 stereocilia, each with 1 channel). This range includes the measured values, but such predictions are uncertain because we do not know single channel currents or the number of channels per stereocilium for turtle utricular hair cells. A related question, as yet unanswered, is whether differ-

ences in stereocilia number will affect overall current-displacement relations.

Taken together, these considerations suggest that type I and type II hair cells will differ in bundle mechanics and maximum mechanotransduction currents because they differ markedly in stereocilia numbers. Thus these two hair cell types may play distinctive roles in encoding head movement.

ACKNOWLEDGMENTS

We thank G. Monk Adams for invaluable technical assistance, Dr. M. H. Rowe for writing the MATLAB routine for coordinate conversions, and J. Xue for the confocal micrograph in Fig. 1A. Drs. R. A. Eatock, J. W. Grant, and M. H. Rowe reviewed the manuscript and provided helpful comments.

GRANTS

This work was supported by National Institute on Deafness and Other Communication Disorders Grant DC-05063 to E. H. Peterson and a Provost's Undergraduate Research Fellowship and Student Enhancement Award to W. J. Moravec.

REFERENCES

- Brichta AM and Peterson EH.** Functional architecture of vestibular primary afferents from the posterior semicircular canal of a turtle, *Pseudemys (Trachemys) scripta elegans*. *J Comp Neurol* 344: 481–507, 1994.
- Denk W, Holt JR, Shepherd GMG, and Corey DP.** Calcium imaging of single stereocilia in hair cells: localization of transduction channels at both ends of tip links. *Neuron* 15: 1311–1321, 1995.
- Fontilla MF and Peterson EH.** Kinocilia heights on utricular hair cells. *Hear Res* 145: 8–16, 2000.
- Houngaard J and Nicholson C.** The isolated turtle brain and the physiology of neuronal circuits. In: *Preparations of Vertebrate Central Nervous System in Vitro*, edited by Jahnsen H. London: John Wiley Ltd, 1990, p. 155–181.
- Howard J, Roberts WM, and Hudspeth AJ.** Mechano-electric transduction by hair cells. *Ann Rev Biophys Chem* 17: 99–124, 1988.
- Jorgensen JM.** The sensory epithelia of the inner ear of two turtles, *Testudo graeca L.* and *Pseudemys scripta*. *Acta Zool* 55: 289–298, 1974.
- Jorgensen JM.** The number and distribution of calyceal hair cells in the inner ear utricular macula of some reptiles. *Acta Zool* 69: 169–175, 1988.
- Jorgensen JM.** Number and distribution of hair cells in the utricular macula of some avian species. *J Morphol* 201: 187–204, 1989.
- Kirkegaard M and Jorgensen JM.** The inner ear macular sensory epithelia of the Daubenton's bat. *J Comp Neurol* 438: 433–444, 2001.
- Lim DJ.** Morphological and physiological correlates in cochlear and vestibular sensory epithelia. *Scan Elec Micro V*: 269–276, 1976.
- Lim DJ.** Fine morphology of the otoconial membrane and its relationship to the sensory epithelium. *Scan Elec Micro III*: 929–938, 1979.
- Lindeman HH.** Regional differences in structure of the vestibular sensory regions. *J Laryngol Otol* 83: 1–17, 1969.
- Moravec WJ and Peterson EH.** Organization of the utricular striola in *Trachemys scripta*: stereocilia counts. *Assoc Res Otolaryngol Abstr* 27: 318, 2004.
- Moravec WJ, Xue J, Rowe MH, and Peterson EH.** Hair bundles of the utricular striola in a turtle, *Trachemys scripta*. *Assoc Res Otolaryngol Abstr* 26: 33, 2003.
- Morita I, Komatsuzaki A, and Tatsuoka H.** The morphological differences of stereocilia and cuticular plates between type-I and type-II hair cells of human vestibular sensory epithelia. *ORL J Otorhinolaryngol Relat Spec* 59: 193–197, 1997.
- Peterson EH, Cotton JR, and Grant JW.** Structural variation in ciliary bundles of the posterior semicircular canal. Quantitative anatomy and computational analysis. *Ann NY Acad Sci* 781: 85–102, 1996.
- Peterson EH and Rowe MH.** Autocorrelation analysis of stereociliary arrays on utricular hair cells. *Soc Neurosci Abstr* 27: 298.22, 2001.
- Rennie KJ and Ricci AJ.** Mechano-electric transduction (MET) and basolateral currents in hair cells of the turtle utricle. *Assoc Res Otolaryngol Abstr* 27: 94, 2004.
- Ricci AJ, Crawford AC, and Fettiplace R.** Tonotopic variation in the conductance of the hair cell mechanotransducer channel. *Neuron* 40: 983–990, 2003.

- Rowe MH and Peterson EH.** Quantitative analysis of stereociliary arrays on vestibular hair cells. *Hear Res* 190: 10–24, 2004.
- Severinsen SA, Jorgensen JM, and Nyengaard JR.** Structure and growth of the utricular macula in the inner ear of the slider turtle *Trachemys scripta*. *J Assoc Res Otolaryngology* 4: 505–520, 2003.
- Silber J, Cotton J, Nam J-H, Peterson EH, and Grant W.** Computational models of hair bundle mechanics: III. 3-D utricular bundles. *Hear Res* In press.
- Werner CF.** Die Differenzierung der Maculae im Labyrinth, insbesondere bei Säugetieren. *Zeitschrift fuer Anatomie und Entwicklungsgeschichte* 99: 696–709, 1933.
- Wersäll J.** Studies on the structure and innervation of the sensory epithelium of the crista ampullares in the guinea pig. *Acta Otolaryngol Suppl* 126: 1–85, 1956.
- Xue J and Peterson EH.** Organization of the utricular striola in *Trachemys scripta*: bundle heights. *Assoc Res Otolaryngol Abstr* 27: 318, 2004.